

A tale of two subunits: co-expression using the dual plasmid approach of the two subunit protein dimethylsulfide monooxygenase from *Hyphomicrobium sulfonivorans*

by

Lydia M. Harris

Honors Thesis (Project)

Appalachian State University

Submitted to

The Honors College

in partial fulfillment of the requirements for the degree of

Bachelor of Science

May, 2018

Approved by:

---

Megen Culpepper, Ph.D., Thesis Director

---

Cara Fiore, Ph.D., Second Reader

---

Jefford Vahlbusch, Ph.D., Director, The Honors College

## Abstract

Dimethylsulfide (DMS) is a volatile organic sulfur compound (VOSC) that makes up about 70% of the atmospheric sulfur flux. Its ability to increase cloud formation, thereby lowering solar radiation, makes it an important gas to investigate for climate cooling options in the battle against global warming. DMS has an active role in linking the global sulfur cycle from the oceans to the atmosphere. There have been few enzymes characterized in the degradation of DMS. Dimethylsulfide monooxygenase is an enzyme that was purified and characterized from the soil bacteria *Hyphomicrobium sulfonivorans* (*H. sulfonivorans*) as a flavin mononucleotide dependent two-component monooxygenase. The A subunit, referred to as DmoA, is a putative monooxygenase, and the B subunit, referred to as DmoB, is a putative flavin reductase. The sequence identity of the *dmoA* gene is known. However, there are two *dmoB* gene candidates on the same operon that encode for putative flavin reductases.

Protein isolation and purification from *H. sulfonivorans* indicates that the DmoA and DmoB subunits coexpress. Attempts to recombinantly express the subunits separately have yielded some promising results, but improvement in regards to protein expression of the B subunit and catalytic activity of the DmoA monooxygenase subunit is needed. DmoA and one of the flavin reductase candidates, referred to as DmoB176, have been co-expressed using the two plasmid approach in BL21DE3 *E. coli*. The *dmoA* gene is located on a plasmid containing ampicillin resistance and the pBR322 replicon, whereas the *dmoB176* gene has been cloned in a vector containing kanamycin resistance and the p15A replicon. The dual plasmids were co-transformed in BL21DE3 *E. coli*, expressed, and purified via affinity chromatography. Initial data confirms expression of the DmoA monooxygenase protein at  $M_r$  of 53 kDa and DmoB176 at  $M_r$  of 19 kDa based of its amino acid sequence. Current research is being performed to

standardize the co-expression procedure in order to measure enzymatic activity downstream.

## **Acknowledgments**

I would first and foremost like to acknowledge Dr. Megen Culpepper, who has invested the past four years to make me a better scientist, critical thinker, and person. Through her guidance, I may one day be able to change my own tire and navigate the world with an atlas. Also, I must recognize the former members of the Culpepper lab who were always willing to lend a hand or answer a question. I would also like to acknowledge Dr. Cara Fiore for taking the time as my second reader to provide feedback on this project.

I would like to thank my family for their constant love and support over the years. No matter how stressed I was, seeing little baby Charles on FaceTime always made things better. Also, thanks to my friends, especially Austin Moore. He has stuck by me during all my highs and lows since we were kids, and is always there for whining and wining.

Finally, I would like to thank the Appalachian State University Honors College, A.R. Smith Department of Chemistry, and the professors in the biology department who provided the foundational knowledge upon which I executed this research.

## **Table of Contents**

<b>Chapter I: Relevance</b>	10
Introduction	10
<i>Global Warming</i>	10
<i>Solar Radiation Management</i>	11
<i>Sulfur Cycle and CLAW Hypothesis</i>	11
<i>Dimethylsulfide</i>	12
<i>Dimethylsulfide Monooxygenase</i>	13
<b>Chapter II: Molecular Cloning</b>	16
Introduction	16
<i>Dual Plasmid Approach</i>	16
Materials and Methods	17
<i>pSAM Stab Culture</i>	17
<i>dmoB176 Polymerase Chain Reaction</i>	18
<i>Agarose Gel Electrophoresis</i>	18
<i>Restriction Enzyme Digestion</i>	19
<i>Ligation</i>	19
Results and Discussion	20
<b>Chapter III: Optimization of Expression and Characterization</b>	23
Introduction	23
<i>Ideal Expression Conditions</i>	24
Materials and Methods	24
Protein Expression	24

<i>dmoB176-pSAM co-expression studies</i>	24
<i>Cell Transformation of dmoB176-pSAM</i>	24
<i>Expression of DmoB176</i>	25
<i>Cell Transformation of dmoA and dmoB176</i>	25
<i>Protein Pilot Co-expression of DmoA-DmoB176</i>	25
<i>Cell Lysis</i>	26
<i>Affinity Chromatography</i>	26
<i>Preparing a 15% SDS-PAGE gel</i>	27
<i>Colony PCR</i>	28
<i>dmoA Gradient PCR</i>	29
<i>dmoA Colony PCR</i>	29
Results and Discussion	30
<i>Co-expression in BL21DE3</i>	31
<i>Colony PCR to monitor dual plasmids</i>	34
<b>Chapter IV: Conclusions</b>	37
Conclusion	37
Future Works	37
Financial Support	39
References	40

## Table of Figures

Figure 1: Chemical structure of DMS	11
Figure 2: Degradation of DMSP to DMS via DMSP lyase	12
Figure 3: Depiction of the formation and degradation of DMS in the marine environment and atmosphere	12
Figure 4: Operon of <i>H. sulfonivorans</i> highlighting the <i>dmoA</i> gene and <i>dmoB</i> gene candidate <i>orf176</i>	14
Figure 5: Model of the oxidation-reduction reaction of the DmoA and DmoB subunits	15
Figure 6: Comparison of the pET-21a and pSAM vectors used for <i>dmoA/dmoB176</i> coexpression	17
Figure 7: Single colony isolation of pSAM in DH5 $\alpha$ on 50 $\mu$ g/mL kanamycin- LB agar	20
Figure 8: 1% Agarose confirming successful amplification of <i>dmoB176</i> over all annealing temperatures in the 55°C to 65°C gradient	20
Figure 9: Comparison of the ligation negative control (left) and successful ligation (right) of <i>dmoB176</i> in pSAM plated on 50 $\mu$ g/mL kanamycin- LB agar	21
Figure 10: Sequencing alignment verifying the insertion of <i>dmoB176</i> in the pSAM vector. The top row is the DNA sequence of <i>dmoB176</i> and the bottom row is the sequence from the ligation reaction.	22
Figure 11: Graph of the logarithmic growing scale for <i>E. coli</i> cells in LB media	24
Figure 12: SDS-PAGE gel of DmoB176/pSAM expression in BL21DE3 <i>E. coli</i> and purification with HiTrap nickel affinity column (GE Biosciences). A buffer gradient with imidazole ranging 20 mM to 500 mM was used for elution.	30
Figure 13: Co-expression of DmoB176 and DmoA at 37°C and 16C in C41DE3 (left) and	

BL21DE3 (right) <i>E. coli</i> . The cells were lysed and the lysates and pellets analyzed at different dilutions with DI H <sub>2</sub> O	31
Figure 14: Trial 1 co-expression of DmoA/DmoB176 in BL21DE3 at 37°C HiTrap purification	32
Figure 15: SDS-PAGE from trial 2 DmoA/DmoB176 BL21DE3 co-expression HiTrap purification	33
Figure 16: SDS-PAGE from trial 3 DmoA/DmoB176 BL21DE3 co-expression HiTrap purification	33
Figure 17: 1% agarose gel electrophoresis of colony PCR at 60°C for DmoB176/DmoA plasmid transformed in BL21DE3 <i>E. coli</i> on 50 ng/μL amp/kan LB-agar	34
Figure 18: 1% agarose gel confirming the success of <i>dmoA E. coli</i> plasmid PCR at all annealing temperatures 55.0°C-65°C	35
Figure 19: 1% agarose gel confirming the success of <i>dmoA</i> BL21DE3 colony and plasmid PCR at 55°C annealing temperature	36



**Table of Tables:**

Table 1: Common vectors with their ori and incompatibility group	16
Table 2: PCR thermocycler conditions for <i>dmoB176</i> amplification	18
Table 3: Sequences and melting temperatures for the <i>dmoA</i> and <i>dmoB176</i> forward and reverse primers	29
Table 4: Comparison of the growth conditions and cells lines assessed for DmoA/DmoB176 co-expression. The optimum conditions are in bold.	29

## **Chapter I: Relevance**

### **Introduction**

#### *Global Warming*

Global warming is a persistent cause of public health concern, with the federal government, researchers from diverse areas of science, and even the public taking an active interest in climate change. The resulting change in weather patterns can pose deleterious effects for natural habitats, wildlife, and human health. Specifically, during the winter months, when temperatures are low, pathogens such as *Phytophthora cinnamon*, *Ophiostoma novoulmi*, and *Ophryocystis elektroschirrha* are killed.<sup>8</sup> Evidence shows that without reversing the warming trends, winter months will become warmer, more pathogens will survive, and an increase in disease spread among plants and animals will likely occur.<sup>8</sup> Warmer temperatures can also affect the survival patterns of mosquitos and ticks, resulting in heightened transmission of Lyme disease and West Nile virus. Efforts to support climate cooling may lead to downstream applications in the defense against these conditions.<sup>4</sup>

#### *Solar Radiation Management*

Although the effects of global warming have been greatly studied, controversy exists on the most effective methods of mitigation. Cost and secondary effects, such as acid rain must be considered with climate cooling strategies. The most obvious way to stop global warming is to cut greenhouse gas emissions, however, globalization, a dependence on fossil fuels and a lack of alternate, clean energy sources require more practical ideas to be pursued.<sup>15</sup> One avenue under consideration is solar radiation management (SRM). This approach involves reflecting radiation away from the atmosphere and back into space, thereby controlling the climate cooling.<sup>24</sup> It has been suggested that the injection of certain aerosols into the atmosphere

increase cloud condensation nuclei (CCN), and thereby reflect radiation back into space.<sup>12</sup> An important element being analyzed for this purpose is sulfur.

### *Sulfur Cycle and CLAW Hypothesis*

Sulfur is an essential element in biochemistry as it is involved in metabolism, catalysis, and structural roles. This diversity in function arises from the vast redox states sulfur can form from highly reduced at -2 to oxidized at +6. Its role in global sulfur cycling includes anaerobic microbe respiration, atmospheric degradation, cloud formation and acid rain. Due to its low vapor pressure, sulfur readily volatilizes and can generate volatile organic sulfur compounds (VOSCs) which have been linked to climate change.<sup>6</sup> Dimethylsulfide (DMS), with the formula  $\text{CH}_3\text{SCH}_3$  (Figure 1), is the most abundant VOSC as it makes up 70% of the global sulfur cycle.<sup>3</sup> DMS is generated from both biological and anthropogenic processes. Anthropogenic processes include the burning of fossil fuels, paper production, and waste water treatment plants. Biological sources of DMS include release by oceanic phytoplankton and coral reefs.<sup>1</sup>

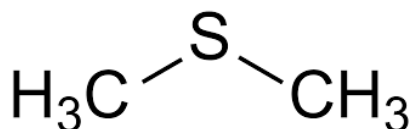


**Figure 1.** Chemical structure of DMS

DMS is a degradation product of dimethylsulphoniopropionate (DMSP). DMSP is enzymatically generated from phytoplankton and its major role is as an osmolyte, meaning it helps maintain the ionic balance of a cell. The degradation of DMSP to DMS by the enzyme DMS lyase (Figure 2) generates the predominate source of biogenic DMS. The formation of DMS by DMSP lyase links the global sulfur cycle from the oceans to the atmosphere in a negative feedback loop described by the CLAW (an acronym for the last names of the authors)

hypothesis (Figure 3). It is hypothesized that water warmed by the sun increases growth of phytoplankton, causing them to produce DMSP, which can be degraded to DMS, thereby increasing the amount of DMS released into the atmosphere.<sup>19</sup> Once in the atmosphere, DMS is oxidized to form sulfate aerosols. Sulfate aerosols in the atmosphere lead to an increase in cloud condensation nuclei (CCN) and droplet number, which in turn enhances cloud albedo, limiting the amount of radiation exposed to the earth. Since less radiation is able to heat the atmosphere, DMS is categorized as a climate-cooling agent.<sup>19, 22</sup> This cooling results in a decrease in phytoplankton growth and the overall negative feedback cycle. Although the conversion of DMSP to DMS by DMSP lyase has been biochemically characterized, the characterization of the breakdown of aquatic or terrestrial DMS is lacking.<sup>19</sup>

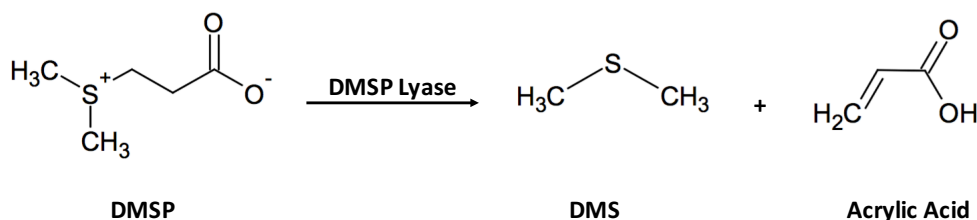


**Figure 2.** Degradation of DMSP to DMS via DMSP lyase<sup>19</sup>

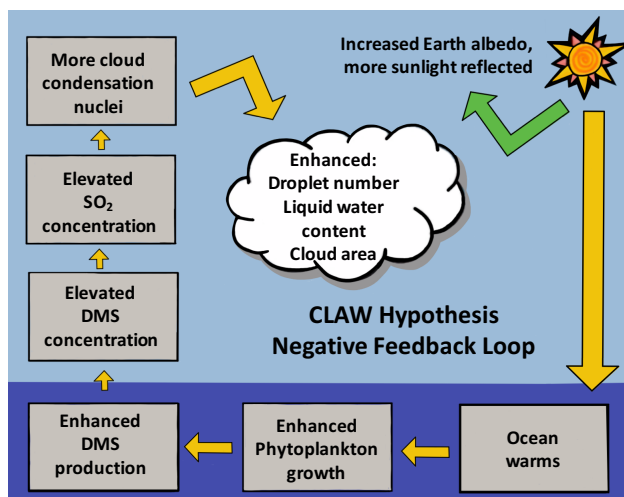


**Figure 3.** Depiction of the formation and degradation of DMS in the marine environment and atmosphere<sup>22</sup>

DMS has been proposed for use in SRM because of its cooling properties. There are concerns, however, that injecting DMS into the atmosphere can lead to adverse effects, mainly acid rain, due to the generation of sulfate aerosol. Studies show that sulfate aerosols added to the stratosphere have longer lifetimes when compared to adding to the troposphere.<sup>18</sup> This longer lifetime decreases the injected amount and may lessen the threats of acid rain. However, before dimethylsulfide can be considered for solar radiation management, its enzymatic metabolic degradation pathway must be characterized.

#### *Dimethylsulfide monooxygenase*

Although DMS is the predominate player in global sulfur cycling, its enzymatic degradation pathway has not been fully elucidated. One enzyme involved in DMS degradation that has been studied to date is the oxidoreductase dimethylsulfide monooxygenase.<sup>2</sup> DMS monooxygenase belongs to a family of two-component FMNH<sub>2</sub>-dependent monooxygenase enzymes.<sup>23</sup> These enzymes contain a reductase subunit that reacts with a nicotinamide adenine dinucleotide (NADH) cofactor to generate a reduced flavin cofactor. The monooxygenase subunit requires the reduced flavin to activate molecular oxygen and the substrate. More specifically, DMS monooxygenase, belongs to one of six flavoprotein monooxygenase subclasses, Class C, in which the enzymes catalyze reactions including hydroxylation, sulfoxidation, and desulfonation. It is believed to be unique compared to the other members of its class because it has increased activity in the presence of divalent metal cofactors (Fe<sup>2+</sup> and Mg<sup>2+</sup>).

*Hyphomicrobium*, *Arthrobacter*, and *Thiobacillus* are species believed to contain DMS monooxygenase enzymes as they are able to grow on DMS as their sole carbon source.<sup>10</sup> The only DMS monooxygenase isolated from its bacterial source comes from the terrestrial bacteria

*Hyphomicrobium sulfonivorans* (*H. sulfonivorans*).<sup>2</sup> It was originally harvested from garden soil and grows as isolates that use DMS, dimethylsulfoxide (DMSO) or dimethylsulfone (DMSO<sub>2</sub>). DMS monooxygenase from *H. sulfonivorans* contains two subunits like other members of this family. A 53 kDa putative monooxygenase subunit, referred to as DmoA, and a 19 kDa flavin reductase subunit, referred to as DmoB. There are two flavin reductase genes located on the *dmo* operon containing the *dmoA* gene encoded by open reading frames (*orf*) 176 and *orf136* (Figure 4).<sup>2</sup> It has been proposed that one of these genes encodes for the native DmoB protein. These proteins will be referred to herein as DmoB176 and DmoB136.<sup>2</sup> Mass spectrometry on natively isolated DMS monooxygenase was unable to definitively identify which reductase is the native binding partner of DmoA; however, since *orf136* is located next to a alkanesulfonate monooxygenase gene, DmoB176 was investigated first. Alkanesulfonate monooxygenase is a well characterized member of the two-component FMNH<sub>2</sub>-dependent monooxygenase enzyme family.<sup>2</sup>

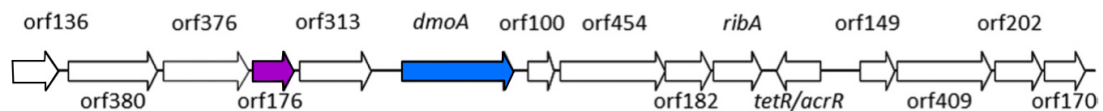


**Figure 4.** Operon of *H. sulfonivorans* highlighting the *dmoA* gene and *dmoB* gene candidate *orf176*<sup>2</sup>

DMS monooxygenase converts DMS and molecular oxygen into methanethiol, water, and formaldehyde at the cost of reduced flavin mononucleotide (FMNH<sub>2</sub>) and reduced nicotinamide adenine dinucleotide (NADH) (Figure 5).<sup>2</sup> DmoB acts as a NADH-dependent FMN reductase, where NADH donates its electrons for the reduction of FMN to FMNH<sub>2</sub>. The FMNH<sub>2</sub> then provides the electrons required for DmoA to convert oxygen and DMS into MT and formaldehyde. From here, formaldehyde can be assimilated to the serine cycle or converted to CO<sub>2</sub>.<sup>2</sup> The results of the native protein expression by Boden et. al. suggests that subunits A

and B tightly associate. Current studies in the Culpepper lab separately express subunits A and B recombinantly in *E. coli*. DmoA expresses in high yield and purity, while both DmoB protein candidates are produced predominately as inclusion bodies. Thus far, there has been no detected MT conversion in DmoA using chemical reductants and only minimal DmoB176 catalytic activity by a standard NADH UV-visible biochemical assay. Based off the observations of Boden et. al. our hypothesis is that DmoA and DmoB form a tight association and the co-expression of both subunits may result in highly active, functional protein. To test this hypothesis, both subunits were co-expressed recombinantly in *E. coli* using the dual plasmid approach incorporating differing origins of replication and antibiotic resistance.<sup>20</sup>

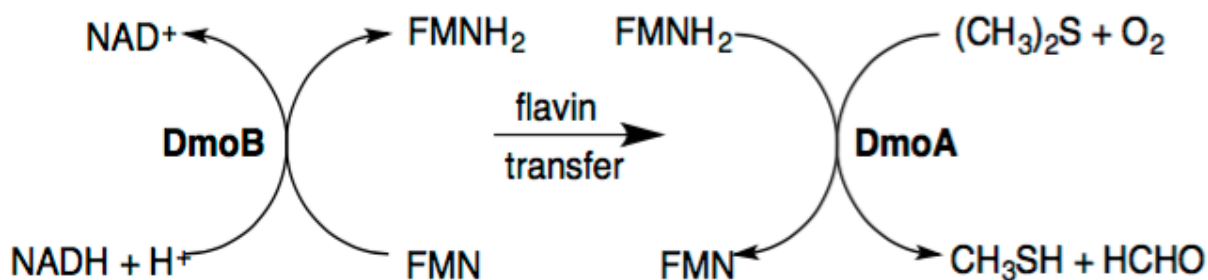


**Figure 5.** Model of the oxidation-reduction reaction of the DmoA and DmoB subunits in DMS monooxygenase<sup>2</sup>

## Chapter II: Molecular Cloning

### Introduction

#### *Dual Plasmid Approach*

Co-expression is a technique often used to enhance the folding of proteins which may have poor solubility and yield when expressed individually. It is also useful in multi-subunit protein expression.<sup>20</sup> The co-expression of both *dmoA* and *dmoB176* genes by the dual plasmid approach was used for this study. The key to this approach is to select a vector with differing origins of replication (ori) and antibiotic resistances of the two gene candidates. A vector is a DNA molecule that acts as a backbone for the gene of interest to allow recombinant replication and expression to occur.<sup>14</sup> The ori is a specific DNA sequence that signals DNA polymerase to initiate replication, and the selectable antibiotic marker confers resistance of the gene of interest.<sup>17</sup> Table 1 outlines common plasmid vectors with their respective antibiotic resistances and origins of replication; those used in these studies are bolded. Co-expression requires selecting two vectors from differing incompatibility groups.<sup>17</sup>

**Table 1.** Common vectors with their ori and incompatibility group<sup>17</sup>

Common Vectors	ORI	Incompatibility Group
<b>pET</b>	<b>pBR322</b>	<b>A</b>
<b>pSAM</b>	<b>p15A</b>	<b>B</b>
pSC101	pSC101	C
pUC	pMB1	A
pR6K	R6K	C

When vectors for co-expression with the same ori are used, the plasmids can compete inside the cell, leading to one being less amplified than the other.<sup>20</sup> To avoid this issue, the



*dmoA* gene was inserted into a pET21a vector with the pBR322 ori, and ampicillin resistance, and the *dmoB176* gene was subcloned into a pSAM vector containing the p15A ori and kanamycin resistance in order to confer co-expression compatibility (Figure 6).<sup>21</sup>

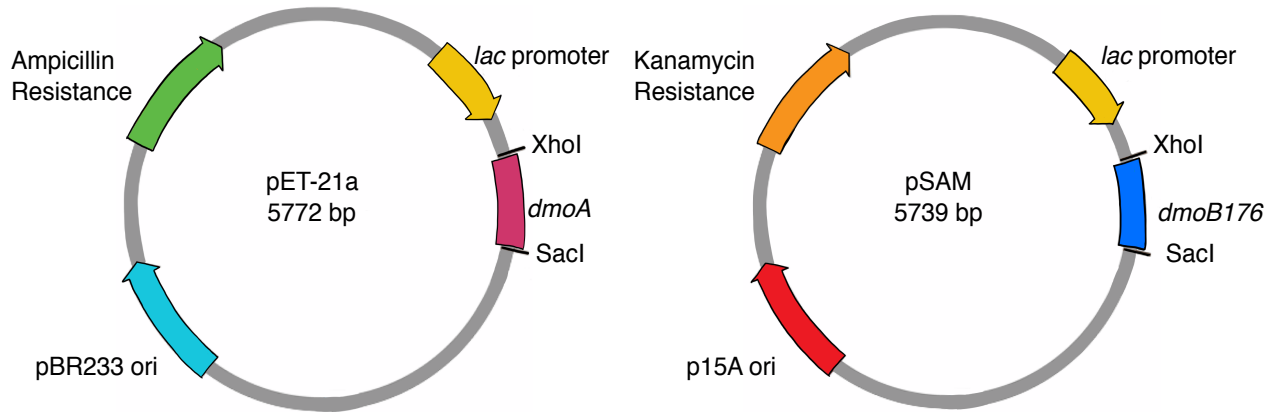


**Figure 6.** Comparison of the pET-21a and pSAM vectors used for *dmoA/dmoB176* coexpression

The Strasbourg lab has demonstrated successful co-expression using this dual vector approach on a two-subunit primase complex in *E. coli*, in which one of the two subunits contained catalytic activity.<sup>5</sup> The Furuya lab co-expressed a flavin reductase gene and a dibenzothiophene monooxygenase, similar to DMS monooxygenase, also using this approach.<sup>7</sup> They selected co-expression due to the large distance between the genes of interest on the operon; they found that genes further apart have greater difficulty expressing separately. Since *dmoB176* is upstream of *dmoA* on the *dmo* operon, and the promoter and *E. coli* cell line used in the Furuya study are the same as those used in this work, the hypothesis gained support.

## Materials and Methods

**pSAM stab culture:** A stab culture of the pSAM vector containing a p15A ori in DH5 $\alpha$  *E. coli* was purchased from Addgene.<sup>21</sup> Under sterile conditions, an inoculation loop was used to streak the pSAM stab culture for colony isolation onto a Luria agar plate containing 50  $\mu$ g/mL kanamycin and incubated overnight at 37°C. A single pSAM colony was then picked under

sterile conditions, and placed in Luria broth (LB) media containing 50 µg/mL kanamycin and incubated overnight at 37°C and 220 rpm. The next day, pSAM plasmid was isolated via a QIAprep Spin MiniPrep kit (Qiagen).

***dmoB176* Gradient PCR (Polymerase Chain Reaction):** PCR was performed on *dmoB176* in a pET-28b (Novagen) vector. Each reaction tube contained; 1X MasterMix (0.05 U/µL Taq DNA polymerase, 4 mM MgCl<sub>2</sub>, 0.4 mM of each dNTP) (Thermo Fisher Scientific), 0.2 µM forward primer (5'-GTCGAGCTCGAGCTGTACCC-3'), 0.2 µM reverse primer (5'-GATCCTCGAGCTCGAGGCTGG-3'), and ~ 50ng *dmoB176* template. The mixture was then split into 5 50-µL aliquots and placed into the thermocycler (MJ Research). A gradient of annealing temperatures was used to amplify the DNA: 55.0°C, 56.7°C, 59.3°C, 62.4°C, and 65.0°C. The PCR program followed the conditions in Table 2 followed by a PCR clean-up (Qiagen) step. The results were analyzed by agarose gel electrophoresis.

**Table 2.** PCR thermocycler conditions for *dmoB176* amplification

Temperature (°C)	Time	Number of Cycles
95	3 min	1
95	30 sec	30
Variable Temperature	45 sec	30
72	1 min	30
72	5 min	1
4	Forever	

**Agarose gel electrophoresis:** A 1% agarose gel matrix was made by combining agarose powder (Fisher Scientific), 1X TE buffer (0.04 M Tris acetate, 1 mM EDTA), and DNA-safe stain (Invitrogen) in a 250-mL Erlenmeyer flask and heated until dissolved. When homogenous, the mixture was poured into the casting mold and an 8-well comb was placed. Once solidified, the samples containing 1X loading dye (10 mM Tris-HCl (pH 7.6) 0.03% bromophenol blue, 0.03% xylene cyanol FF, 60% glycerol 60 mM EDTA) (Thermo Fisher

Scientific), as well as the molecular weight marker (GeneRuler 1 kb) were loaded. The gel was run for 60 minutes at 140 V and was then analyzed by UV light (FOTODYNE).

**Restriction enzyme digest:** In separate 1.5-mL Eppendorf tubes, the pSAM plasmid and *dmoB176* PCR product were combined with CutSmart buffer (50 mM potassium acetate, 20 mM tris-acetate, 10 mM magnesium acetate, 100 µg/mL BSA, pH 7.9) (New England BioLabs/NEB), 2 units/µL SacI (NEB), 2 units/µL XhoI (NEB), and nuclease free water. Both mixtures were digested at 37°C for at least 15 minutes then analyzed via agarose gel electrophoresis.

**Ligation:** In a 1.5-mL tube, digested pSAM vector and digested *dmoB176* PCR product were combined with 50mM Dithiothreitol (DTT) (Thermo Fisher Scientific), 1X ligase buffer (50 mM Tris-HCl, 10 mM MgCl<sub>2</sub>, 10 mM Dithiothreitol 1 mM ATP, pH 7.5) (NEB), and ligase (NEB) and incubated at 16 °C overnight. The mixture was transformed in *E. cloni* competent cells (Lucigen), plated on a 50 µg/mL kanamycin-LB plate, and incubated at 37°C overnight. A starter culture was made with sterile LB media, 50 µg/mL kanamycin, and a single colony from the plate. After an overnight incubation at 37°C at 220 rpm, the cell pellet was isolated, resuspended, and the plasmid was isolated by QIAprep Spin MiniPrep kit (Qiagen).

The ligation reactions were tested for insert by small scale restriction enzyme digestion. The *dmoB176*/pSam ligation plasmid, 2 units/µL SacII (NEB), 2 units/µL XhoI, and CutSmart (50 mM potassium acetate, 20 mM tris-acetate, 10 mM magnesium acetate, 100 µg/mL BSA, pH 7.9) buffer (NEB) was digested at 37°C for 15 minutes. The digested vector was analyzed via agarose gel electrophoresis and plasmids containing a band corresponding to the *dmoB176* insert were sent for Sanger sequencing (Eurofins genomics) for verification.

## Results and Discussion

The pSAM vector in DH5 $\alpha$  *E. coli* cells was successfully streaked on a kanamycin resistant LB agar plates and single colonies were isolated (Figure 7). The *dmoB176* gene was amplified successfully by gradient PCR as demonstrated in the gel in Figure 8. Under the experimental conditions in Table 2, *dmoB176* shows amplification under all of the annealing temperatures ranging 55°C to 65°C. Since *dmoB176* is 531 bp, the band at ~500 bp in each lane indicates that PCR was successful (the PCR primers were compatible) over all variable annealing temperatures.

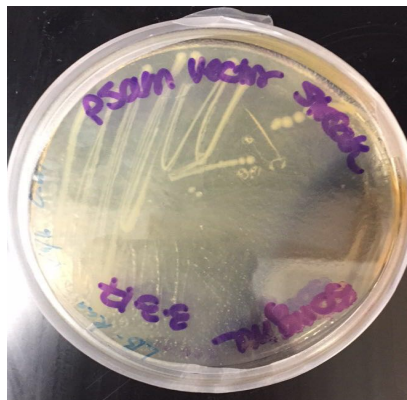


**Figure 7.** Single colony isolation of pSAM in DH5 $\alpha$  on 50  $\mu$ g/mL kanamycin- LB agar

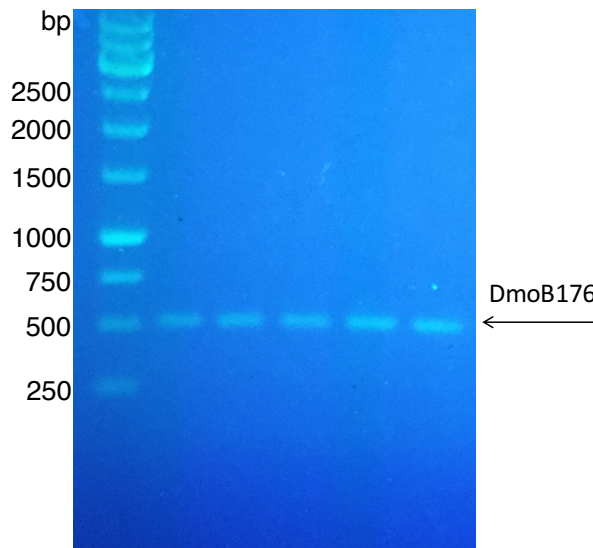


**Figure 8.** 1% Agarose confirming successful amplification of *dmoB176* over all annealing temperatures in the 55°C to 65°C gradient

After PCR amplification, both the *dmoB176* and pSAM were digested with XhoI and SacI restriction endonucleases. The digestion was proven successful after analysis via agarose gel electrophoresis.

Digested insert (*dmoB176*) and vector (pSAM) were joined together via ligation. The ligation reactions were transformed in the DH5 $\alpha$  competent *E. coli* cell line. A negative control, consisting of cut vector, was also plated. Both the negative control and gene/vector ligation reactions were performed at 16°C are shown below (Figure 9). The negative control of the digested insert was expected to produce no colonies as it contains no insert and therefore is not circular. We observed no colonies on the negative control, indicating the colonies from the ligation mixture likely contained our *dmoB176* gene.

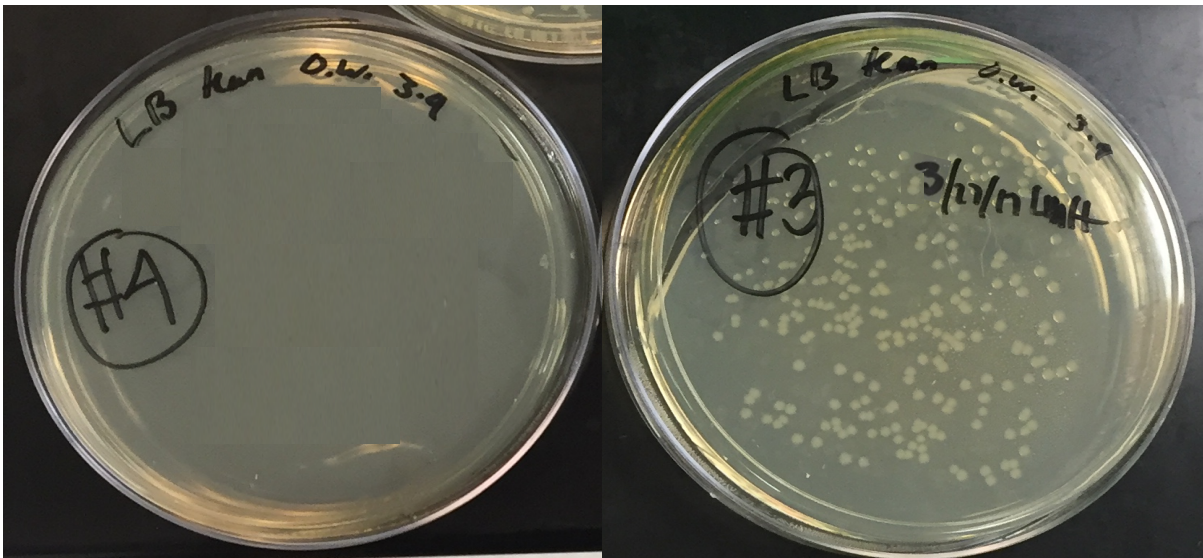


**Figure 9.** Comparison of the ligation negative control (left) and successful ligation (right) of *dmoB176* in pSAM plated on 50  $\mu$ g/mL kanamycin- LB agar

Plasmids generated from the transformed ligation reaction were digested with XhoI and SacII. A SacII site was engineered into the pSAM vector to screen ligation conditions.<sup>21</sup> The digested ligation was analyzed with gel electrophoresis and was a success due to a band at the

expected size of 510 bp corresponding to the DNA sequence of *dmoB176*. In order to verify the insert was present in the pSAM vector, the plasmids were analyzed by Sanger sequencing. The ligation reaction sequence was compared to the DNA sequence of *dmoB176* (Figure 10), which showed 100 % alignment confirming the ligation worked. The *dmoB176*/pSAM vector was then used for subsequent protein expression screening.

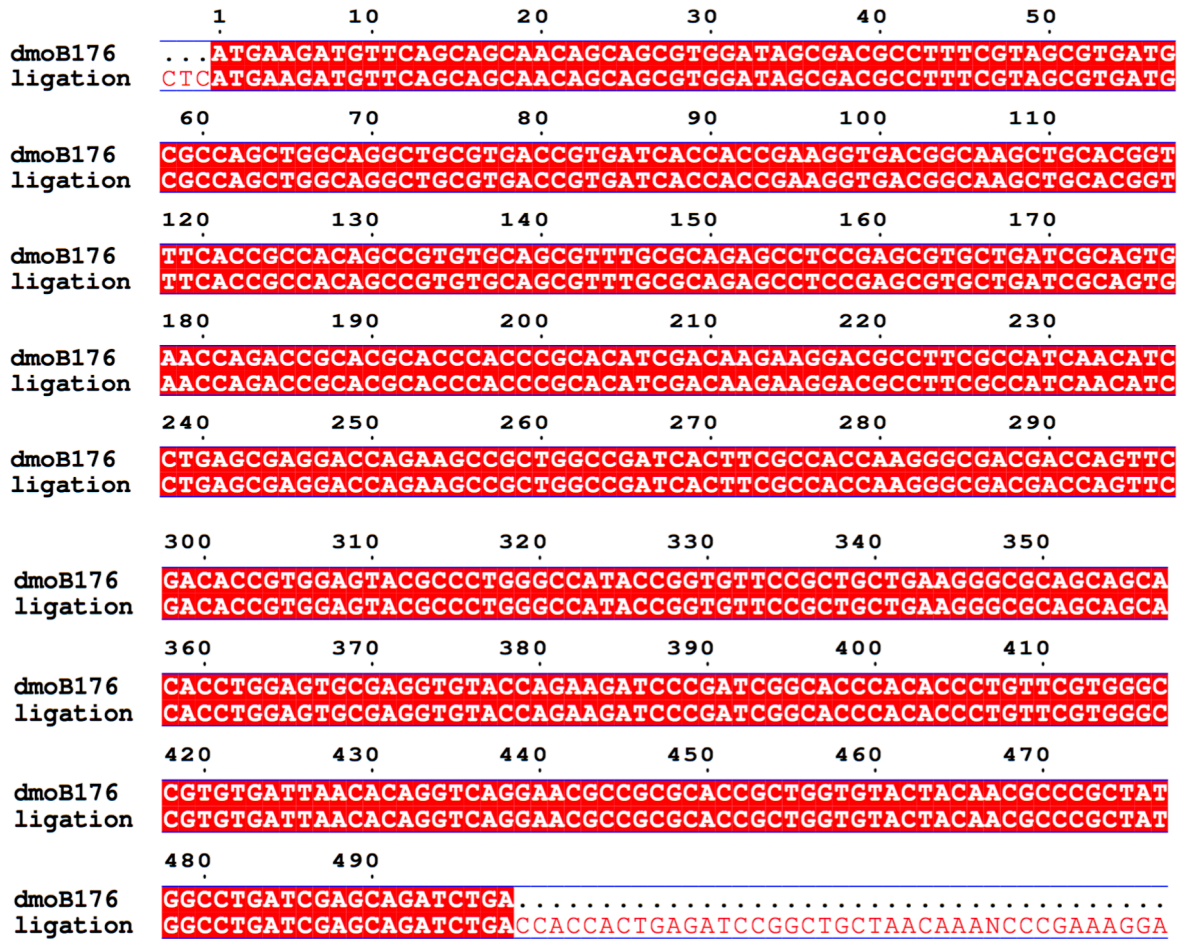


**Figure 10.** Sequencing alignment verifying the insertion of *dmoB176* in the pSAM vector. The top row is the DNA sequence of *dmoB176* and the bottom row is the sequence from the ligation reaction.

### **Chapter III: DmoA/DmoB176 Protein Expression Optimization and Characterization**

#### **Introduction:**

Recombinant protein expression is performed on genes that are controlled by a single promoter. A promoter is a sequence of DNA that initiates transcription of the genes of interest. RNA polymerases attach to the promoter, separate the two strands of DNA, and transcribe the nucleotides of the DNA template strand to RNA. Translation occurs when three nucleotides, or codons, are translated into amino acids by ribosomes, forming the protein sequence.<sup>9</sup> In prokaryotes, transcription and translation are coupled and occur at the same time.

The way in which a protein is expressed depends on the structure of the operon containing the gene of interest. The *dmoA* and *dmoB176* genes are present on the *lac* operon with a T7 promoter. The *lac* operon is needed for bacteria, such as *E. coli*, to metabolize lactose, a sugar used when glucose is deficient. When there is no lactose, a repressor binds to the operator and prevents translation. However, when there is lactose present, allolactose binds to the repressor, removes it from the operator, and allows protein synthesis to occur.<sup>9</sup> When co-expressing DmoA and DmoB176, Isopropyl  $\beta$ -D-1-thiogalactopyranoside (IPTG), an allolactose mimicking sugar, is used for induction. This then stimulates translation of the genes of interest.<sup>9</sup>

Prior to induction, protein expression takes place in liquid LB media, which provides nourishment for *E. coli* replication. *E. coli* cells grow exponentially on a log scale and can be monitored by measuring the optical density at 600 nm (OD<sub>600</sub>). Once they reach an OD<sub>600</sub> of 0.4-0.6, they are in mid-log phase, meaning the cells are rapidly reproducing and should be induced with a sugar to amplify protein production, and thereby amplify yield (Figure 7).

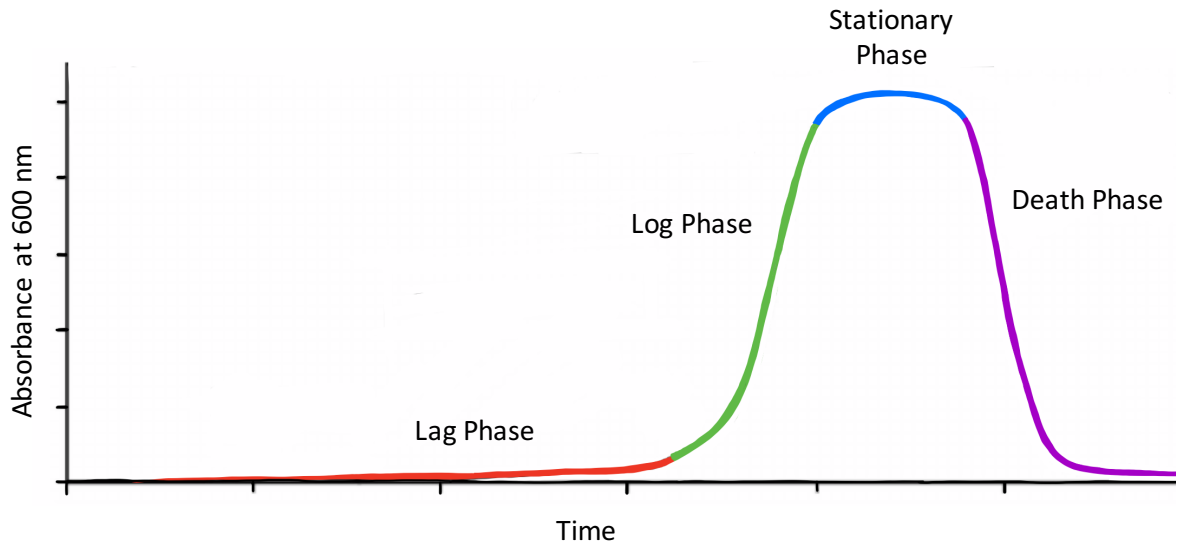


**Figure 11.** Graph of the logarithmic growing scale for *E. coli* cells in LB media

### *Ideal Expression Conditions*

Past work in the Culpepper lab has included optimizing growth conditions for the individual expression of DmoA and DmoB176. Previously, DmoA and DmoB176 have been expressed separately in different competent *E. coli* cell lines at different temperatures. These conditions were used to investigate co-expression of both subunits. In addition, the expression of DmoB176 in the pSAM vector was performed to ensure expression of the protein by itself. The efficacy of competent cell lines, growth temperatures, and growth durations were all explored.

### **Materials and Methods**

#### *Protein Expression*

##### *dmoB176-pSAM expression studies:*

**Cell Transformation of *dmoB176-pSAM*:** Under sterile conditions, *dmoB176-pSAM* plasmid was added to BL21DE3 *E. coli* competent cells (Lucigen) in a 1.5-mL Eppendorf tube and incubated on ice for thirty minutes. The tube was then heat shocked in a water bath at 42°C for 45 seconds, followed by another two-minute incubation on ice. SOC recovery media (Lucigen)



was added and the cells incubated at 37°C at 220 rpm for one hour. Under sterile conditions, the mixture was plated on LB-agar containing 50 µg/mL kanamycin, and incubated overnight at 37°C.

**Expression of DmoB176:** Aseptically, a starter culture was prepared with LB media, a single colony from the BL21DE3 cell transformation, and 50 µg/mL kanamycin. It was incubated overnight at 37°C and 220 rpm. A 2.5-L flask (Thomson Ultra Yield Solution) containing 1.0 L sterile LB media, 50 µg/mL kanamycin and starter culture was incubated at 37°C and 220 rpm. The culture was monitored by UV-VIS spectrophotometry (Agilent Technologies) until the optical density at 600 nm (OD<sub>600</sub>) was 0.4-0.6. The culture was induced with 1 mM isopropyl-β-D-thiogalactopyranoside (IPTG) sugar (Chem-Impex Int'l. Inc.) and grown at 37°C and 220 rpm for three hours. The cells were then harvested via centrifugation (4,200 rpm, 4°C, 15 minutes) and stored at -20°C for future use.

*Dual plasmid dmoB176-pSAM and dmoA-pet21a co-expression studies:*

**Cell Transformation of *dmoA* and *dmoB176*:** Under sterile conditions, *dmoA-pET21a* and *dmoB176-pSAM* plasmid were added to BL21DE3 *E. coli* competent cells (Lucigen) in a 1.5-mL Eppendorf tube and incubated on ice for thirty minutes. The dual plasmid transformation required 50 ng of each plasmid to obtain single colonies. The tube was then heat shocked in a water bath at 42°C for 30 seconds, followed by another two-minute incubation on ice. SOC recovery media (Lucigen) was added and the cells incubated at 37°C at 220 rpm for one hour. Using sterile conditions, the mixture was added to an LB agar plate containing both 50 µg/mL kanamycin and 100 µg/mL ampicillin, and incubated overnight at 37°C before long-term storage at 4°C. Cell transformations using C41DE3 (Lucigen) and SHuffle T7 (NEB biosciences) cells followed the same procedure.

**Protein Pilot Co-expression of DmoA and DmoB176:** Under sterile conditions, starter cultures were made containing LB media, 1 colony from the cell transformation in either BL21DE3, C41DE3, or SHuffle T7 cells (in order to screen for expression under different cell lines), and 50 µg/mL kanamycin and 100 µg/mL ampicillin, followed by incubation overnight at 37°C and 220 rpm. Two 250-mL Erlenmeyer flasks per cell line (6 total flasks) containing 100 mL sterile LB media, 50 µg/mL kanamycin, 100 µg/mL ampicillin, and starter culture were incubated at 37°C and 220 rpm until the optical density at 600 nm (OD<sub>600</sub>) was 0.4-0.6. One culture was induced with 1 mM isopropyl-β-D-thiogalactopyranoside (IPTG) sugar and grown at 37°C at 220 rpm for three hours. The other culture was placed at 4°C for three hours, induced with 1 mM IPTG, and grown overnight at 16°C and 220 rpm. The cell harvest and lysis were performed as listed under “Expression of DmoB176” (above). Large scale co-expression studies also utilized this method.

#### *Protein Purification and Analysis*

**Cell Lysis:** The cell pellet was resuspended in 50mM Tris, 500 mM NaCl, pH 8.0 buffer containing a protease inhibitor cocktail powder (ThermoFisher Scientific) and lysozyme (ThermoFisher Scientific). The mixture was rocked at room temperature for 15-30 minutes. The cells were lysed via sonication (Qsonica) for ten minutes (10 seconds on, 30 seconds off, amplitude 40). The crude lysate mixture was centrifuged for 45 minutes at 4°C and 11,000 rpm. The crude lysate was collected, followed by purification via HiTrap Nickel affinity chromatography (GE Healthcare) described below. All cell pellets followed this protocol with the exception of the large-scale growth, which removed the addition of lysozyme.

**Affinity Chromatography:** Two buffers were prepared; buffer A: 50 mM Tris pH 8.0, 500 mM NaCl, 20 mM imidazole, buffer B: 50 mM Tris pH 8.0, 500 mM NaCl, 500 mM imidazole.

Before each purification, a 5-mL HiTrap Nickel affinity column (GE Healthcare) that recognizes the His<sub>6</sub>-tag on the plasmid was washed with 5 column volumes (CV) of DI H<sub>2</sub>O, followed by 5 CV 0.05 M EDTA buffer, and an additional 5 CV of DI H<sub>2</sub>O. 0.5 CV of 0.1 M NiSO<sub>4</sub> was applied to the column and then rinsed with 5 CV DI H<sub>2</sub>O. The column was then equilibrated with 10 CV of buffer A.

A blank run was performed on the column at a flow rate of 1 mL/min with 10 CV DI H<sub>2</sub>O, 10 CV buffer B, 20 CV buffer A. At 4°C, the crude lysate was loaded onto the column at 1 mL/min and washed with 40 CV buffer A. A linear gradient from 0% to 100% buffer B over 15 CV was performed at 1 mL/min and fractions were collected. The column was washed with 10 CV buffer A, followed by 30 CV DI H<sub>2</sub>O. The results were analyzed via SDS-PAGE.

**Preparing a 15% SDS-PAGE gel:** The gel casting apparatus (BioRad) was constructed by rinsing two glass plates in 20% ethanol, placing them together and securing them to a rubber pad to prevent leakage. Two 15% SDS-PAGE resolving gels (0.38 M Tris-HCl pH 8.8 buffer, 37% deionized water, 14.4% acrylamide (BioRad), 0.05% ammonium persulfate (APS) (BioRad), 0.10 % sodium dodecyl sulfate (SDS), and 1 % tetramethylethylenediamine (TEMED) (BioRad)) were prepared. The liquid mixture was inverted several times and applied between a gap in the glass plates. N-butanol was added to the top of the solution and removed once the gel polymerized.

Stacking gels (0.12 M Tris-HCl pH 6.8 buffer, 60% deionized water, 5.15% acrylamide, 0.05% APS, 0.12% SDS, and 2% TEMED) were prepared and the mixture was applied to the gel plates, followed by the insertion of the well comb. Once hardened, the well comb was removed and the plates were placed in the electrophoresis container filled with running buffer (25 mM Tris, 192 mM glycine, 0.1% SDS at pH 8.3). Reducing buffer (312.5

mM Tris-HCl pH 6.8, 50% glycerol, 0.25% bromophenol blue, 10% SDS, 12.5%  $\beta$ -mercaptoethanol) was added to the protein samples and boiled for five minutes before being loaded on to the gels.

The gels were run at 200V for approximately 50 minutes followed by incubation with Coomassie staining solution (11.1 M methanol,  $3.4 \times 10^{-3}$  M Coomassie brilliant blue stain, 9.6 M glacial acetic acid) on a rocker for 10 minutes. They were then transferred into a destain solution (9.9 M methanol, 1.2 M glacial acetic acid) until protein bands were visible.

**Colony PCR:** PCR was performed on colonies from the *dmoB176/dmoA* co-transformation in BL21DE3 cells. In an Eppendorf tube, MasterMix (0.05 U/ $\mu$ L Taq DNA polymerase, 4 mM MgCl<sub>2</sub>, 0.4 mM of each dNTP) (Lucigen), 0.2  $\mu$ M *dmoB176* forward primer, 0.2  $\mu$ M *dmoB176* reverse primer, 0.2  $\mu$ M *dmoA* forward primer, and 0.2  $\mu$ M *dmoA* reverse primer (Table X), and nuclease free water were combined and mixed by pipetting up and down. The mixture was then split into 15 10- $\mu$ L aliquots. A single colony from the dual antibiotic plate was picked with a pipette tip, swirled in the PCR mix and then touched to a new, gridded, 50  $\mu$ g/mL kan/100  $\mu$ g/mL amp LB-agar plate. The plate was incubated at 37°C overnight. The tubes were placed into the thermocycler (MJ Research), and run under the conditions outlined in Table 2 described in section “*dmoB176 Gradient PCR.*” The PCR products were then analyzed via agarose gel electrophoresis

***dmoA Gradient PCR:*** *dmoA* was amplified using the procedure in “*dmoB176 Gradient PCR.*” The primers used were 0.2  $\mu$ M *dmoA* forward primer and 0.2  $\mu$ M *dmoA* reverse primer (Table 3).

***dmoA Colony PCR:*** *dmoA* was transformed in the BL21DE3 *E. coli* cell line and plated on 100  $\mu$ g/mL amp LB-agar. Colonies were picked, inoculated in LB media with 100  $\mu$ g/mL

ampicillin, and a plasmid MiniPrep (Qiagen) was performed. MasterMix, 0.2  $\mu$ M *dmoA* forward primer, and 0.2  $\mu$ M *dmoA* reverse primer (Table 3) was combined and mixed by pipetting up and down. *dmoA*/BL21DE3 plasmid was added to four aliquots. Four *dmoA*/BL21DE3 colonies were picked, swirled in four individual aliquots that did not contain plasmid, and touched on a new, gridded, 100  $\mu$ g/mL amp LB-agar plate. The plate incubated overnight at 37°C. The tubes were placed in the thermocycler and PCR was performed using the conditions outlined in Table 2 (section *dmoB176 Gradient PCR*) with an annealing temperature of 55.0°C. The results were analyzed via agarose gel electrophoresis.

**Table 3.** Sequences and melting temperatures for the *dmoA* and *dmoB176* forward and reverse primers

Primer	Sequence	Melting Temperature (°C)
<i>dmoA</i> Forward	5'-GATCGAGCTCATGAAACGTATCGTTC-3'	64.6
<i>dmoA</i> Reverse	5'-GATCCTCGAGCTCAGCCACCG-3'	68.4
<i>dmoB176</i> Forward	5'-GTCGAGCTCGAGCTGTACCC-3'	64.6
<i>dmoB176</i> Reverse	5'-GATCCTCGAGCTCGAGGCTGG-3'	67.7

## Results and Discussion

Single expression of DmoB176 in the pSAM vector was performed in BL21DE3 cells for verification purposes; past works in the Culpepper lab have expressed DmoB176 in the pET-28b vector. After growth, the cells were harvested, lysed, and purified using HiTrap nickel affinity chromatography. The protein load band corresponds to the flow through fractions after loading the lysate and the wash is the fraction after the column is washed with buffer to remove non-specific protein binding. SDS-PAGE analysis of the elution fractions shows a faint band at ~19 kDa, indicating that the pSAM vector is able to express DmoB176 (Figure 12).

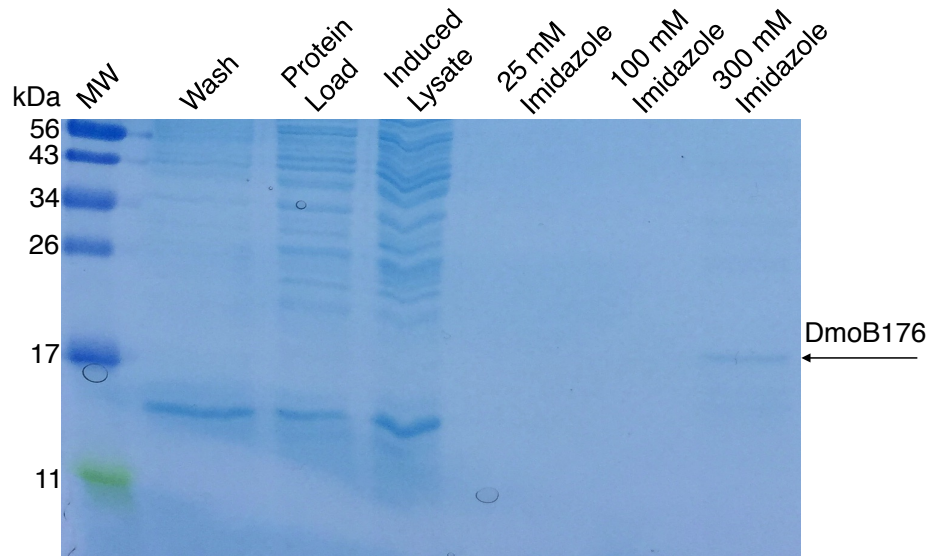


**Figure 12.** SDS-PAGE gel of DmoB176/pSAM expression in BL21DE3 *E. coli* and purification with HiTrap nickel affinity column (GE Biosciences). A buffer gradient with imidazole ranging 20 mM to 500 mM was used for elution. A protein band at MW of ~19kDa was present in the high imidazole fractions corresponding to DmoB176 expression.

Pilot co-expression studies were performed using the conditions presented in Table 4. After harvesting, lysing, and analyzing the cells from each growth, co-expression using BL21DE3 *E. coli* and Growth Condition A (Table 4) was deemed optimal as determined by SDS-PAGE. Figure 13 compares co-expression in C41DE3 (left) and BL21DE3 cells (right) both grown at 37°C for three hours after IPTG induction. The bands at ~55 kDa in the BL21DE3 gel were more prominent than those in the C41DE3 gel, indicating that cell line was favorable for expression of DmoA; it was selected for further co-expressions. Both gels showed intense bands at ~17 kDa, referred to herein as DmoX. Since DmoB176 is an assumed 19 kDa protein, the DmoX band at ~17 kDa observed in Figure 13 was sequenced by Mass Spectrometry (UNC-Chapel Hill) for identification. The mass spectrometry results indicated the protein band DmoX was as lysozyme added during the lysis procedure, not DmoB176. To test this theory lysozyme was removed from subsequent lysis protocols and the 17 kDa band was eliminated, confirming that the band was not DmoB176.

**Table 4.** Comparison of the growth conditions and cells lines assessed for DmoA/DmoB176 co-expression. The optimum conditions are in bold.

<i>E. Coli</i> competent cell line	Growth Conditions A	Growth Conditions B
<b>BL21DE3</b>	<b>37°C for 3 hours at 220 rpm</b>	1 hour cold shock (4°C), 16°C overnight at 220 rpm
C41DE3	37°C for 3 hours at 220 rpm	1 hour cold shock (4°C), 16°C overnight at 220 rpm
T7 SHuffle	37°C for 3 hours at 220 rpm	1 hour cold shock (4°C), 16°C overnight at 220 rpm

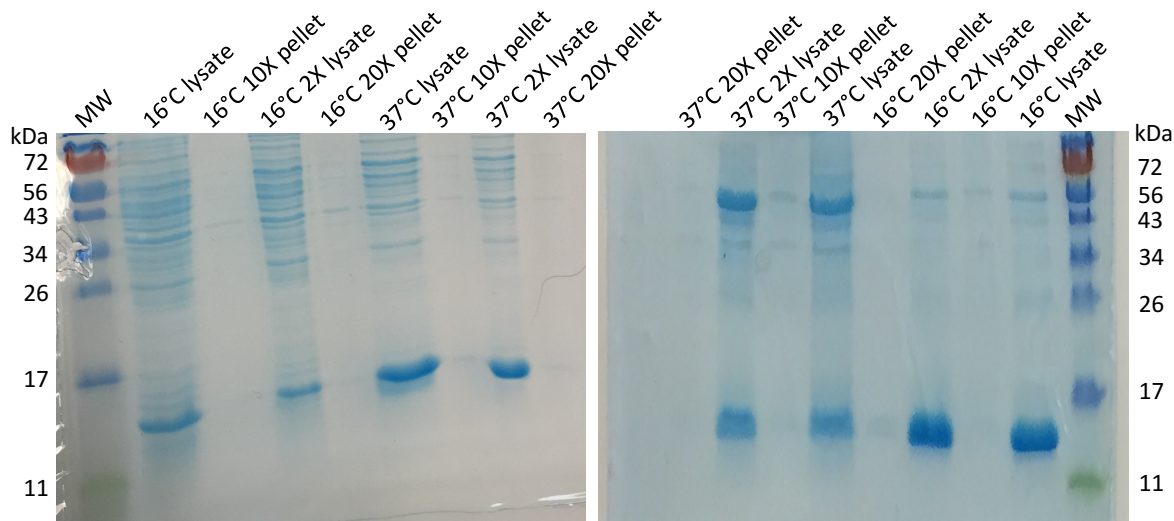


**Figure 13.** Co-expression of DmoB176 (19 kDa) and DmoA (53 kDa) at 37°C and 16°C in C41DE3 (left) and BL21DE3 (right) *E. coli*. The cells were lysed and the lysates and pellets analyzed at different dilutions with DI H<sub>2</sub>O. The band at ~15kDa corresponds to lysozyme added during the lysis procedure.

#### *Co-expression in BL21DE3*

In three separate large-scale co-expressions of the *dmoA* and *dmoB176* genes, different results were produced. Each co-expression was conducted in BL21DE3 cells at 37°C for three hours and purified with HiTrap nickel affinity. After SDS-PAGE gel analysis, Trial 1 produced nearly stoichiometric amounts of the DmoA and DmoB176 proteins. It also yielded relatively high purity after additional purification by size exclusion chromatography (not shown);

although the elution profile from the sizing column did not match the anticipated molecular weight of the co-expressed proteins based on molecular weight standards. These results were promising because not only were similar amounts of each protein expressed, they were eluting together, indicating a possible interaction.

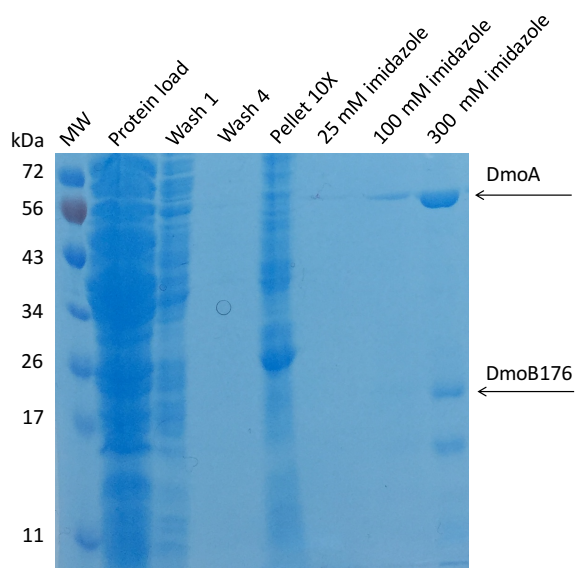


**Figure 14.** Trial 1 co-expression of DmoA/DmoB176 in BL21DE3 at 37°C HiTrap purification

In trial 2, DmoA was over-expressed at 55 kDa and no bands near 19 kDa were present on the gel; therefore, DmoB176 was determined to not be expressed (Figure 15). Co-expression trial 3 was performed using colonies from the same BL21DE3 *dmoA/dmoB176* 100  $\mu\text{g/mL}$  Amp/50  $\mu\text{g/mL}$  Kan plate as in trial 2. DmoA was once again over-expressed at 55 kDa; however, there was also a weak 19 kDa band on the gel assumed to be DmoB176 (Figure 16). In order to reproduce the favorable results from trial 1, co-expression was stalled in order to develop a procedure for consistent dual transformation of the *dmoA* and *dmoB176* plasmids in BL21DE3 cells.



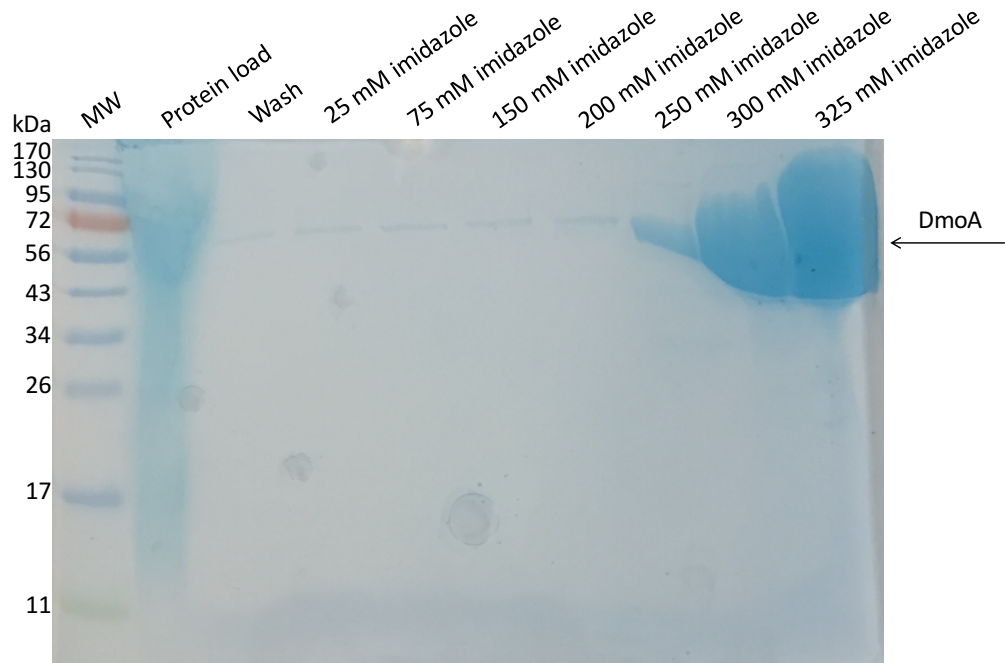


**Figure 15.** SDS-PAGE from trial 2 DmoA/DmoB176 BL21DE3 co-expression HiTrap purification

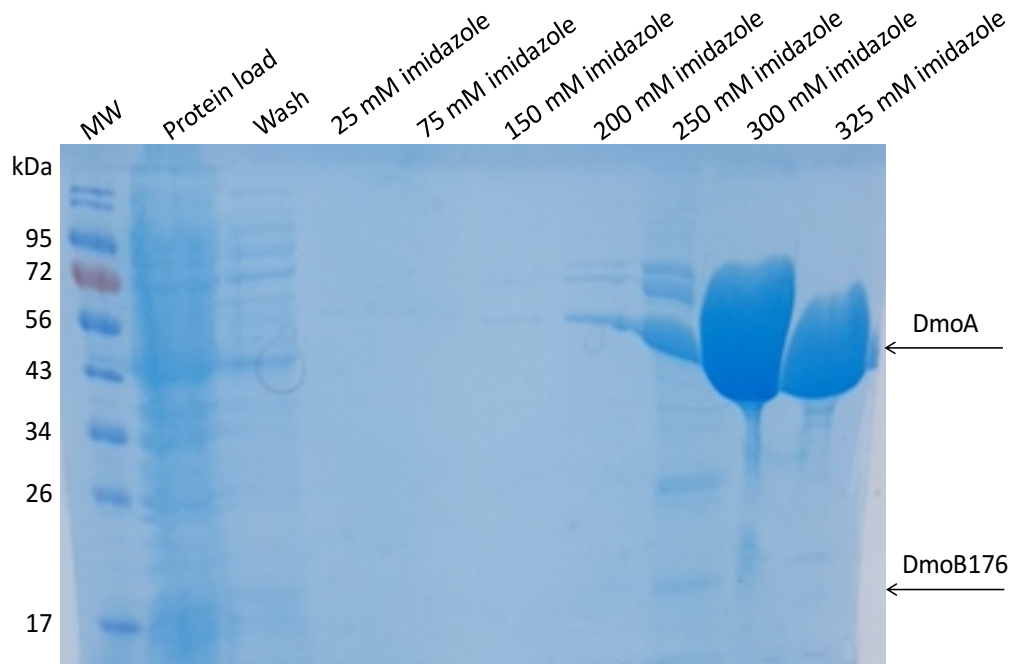


**Figure 16.** SDS-PAGE from trial 3 DmoA/DmoB176 BL21DE3 co-expression HiTrap purification

### Colony PCR to monitor dual plasmids

Based on previous experimentation, it was found that PCR of both *dmoB176* and *dmoA* genes was successful at annealing temperatures of 55°C - 65°C. Therefore, colony PCR was performed at an annealing temperature of 60°C using primers specific for both *dmoB176* and *dmoA* genes in the reaction mixture. 15 colonies were picked from the same plate used for the inoculum in co-expression trials 2 and 3 and underwent PCR. Analysis was performed via agarose gel electrophoresis (Figure 17). For all lanes except 12, a band at 500 bp corresponding to *dmoB176* was present. Lanes 13-15 also revealed a primer dimer at approximately 50 bp. No bands appeared at 1500 bp corresponding to the *dmoA* gene. This meant that the *dmoB176* gene was present in the colonies used for inoculation but no or weak co-expression was observed. Since DmoA was expressed in all three trials, and was expected to be on the gel, the PCR conditions were further analyzed.

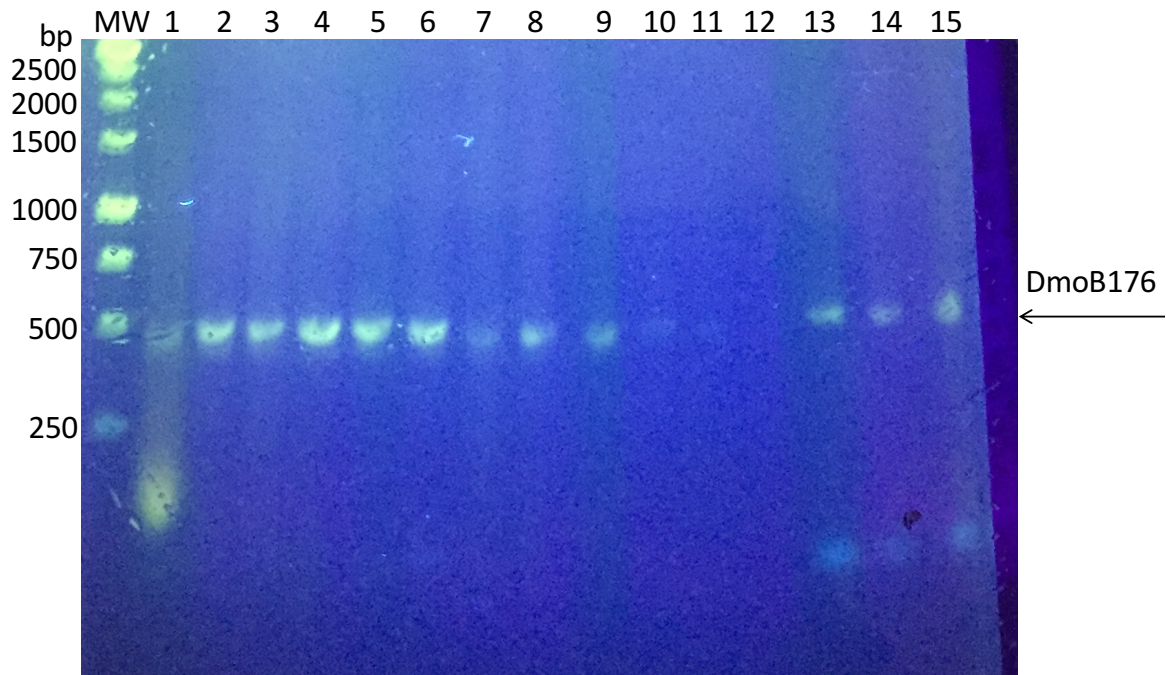


**Figure 17.** 1% agarose gel electrophoresis of colony PCR for *dmoB176/dmoA* plasmid transformed in BL21DE3 *E. coli*.

In order to test the efficacy of the *dmoA* primers, PCR was performed on *dmoA* plasmid

from *E. coli* competent cells. A gradient of annealing temperatures was used from 55°C-65°C. Analysis was done via agarose gel electrophoresis (Figure 18). A band at approximately 1500 bp was present in each lane, indicating that the primers worked for *dmoA* PCR at all temperatures. Since the band at 55.0°C was the most prominent, this temperature was selected for future experimentation.

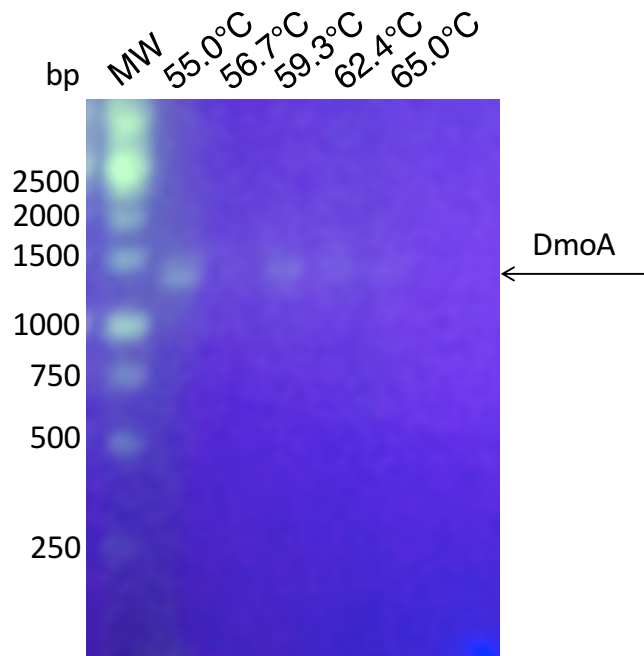


**Figure 18.** 1% agarose gel confirming the success of *dmoA* *E. coli* plasmid PCR at all annealing temperatures 55.0°C-65°C

It was hypothesized that the *dmoA* gene may not be as compatible with the BL21DE3 cells as the *dmoB176* gene, which would explain its absence in the dual plasmid colony PCR (Figure 17). To test this, *dmoA* plasmid was solely transformed in the BL21DE3 cell line and isolated (Qiagen). PCR was repeated on both the plasmids isolated from BL21DE3 and colonies from the transformation containing only the *dmoA* gene. Figure 19 shows the results of PCR for the colonies (C1-4) and the plasmids (P1-4). Although each lane has a band at 1500 bp, the bands in P1-4 from the plasmid PCR products were most prominent. This rejected the prediction that *dmoA* had a lower affinity for the BL21DE3 plasmid.

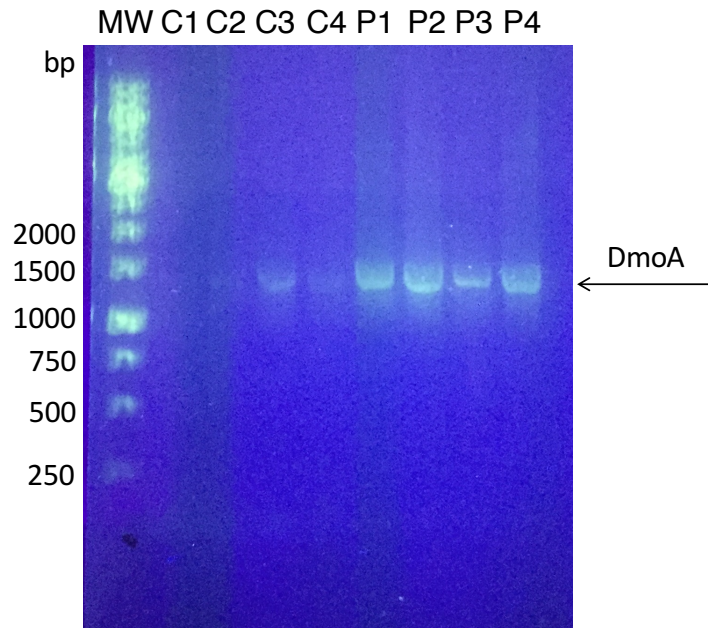


**Figure 19.** 1% agarose gel confirming the success of *dmoA* BL21DE3 colony and plasmid PCR at 55.0°C annealing temperature

The results from the colony screening were inconclusive. The reason as to why DmoA protein was over-expressed (Figure 16, 17), yet not present in the DNA gels from the dual plasmid colonies (Figure 18) could not be determined. There was also no concrete reason as to why DmoB176 was only expressed in a stoichiometric amount to DmoA in one expression trial yet produced little to no yield in the other two. Therefore, in order to solidify a protocol that would ensure the expression of the same amount of DmoA and DmoB176 every time, further troubleshooting is needed. For instance, running the colony PCR in reactions where the *dmoB176* and *dmoA* specific primers are separated, or generating competent cells containing one gene then transforming the other gene into these cells. Lastly, screening additional cell lines that may regulate the lac operon such as BL21plysS, assist in disulfide bond formation such as Rosetta, or make expression tunable such as in Lemo21(DE3) should be performed.

## Chapter IV: Conclusions

### *Conclusions*

The insertion of the *dmoB176* gene into the pSAM vector with kanamycin antibiotic resistance was a success; this made *dmoB176* compatible for co-expression using the multiple vector approach. The hypothesis that DmoA and DmoB176 form a tight association which may increase activity was neither supported nor rejected. The subunits were successfully co-expressed in stoichiometric amounts in one of three trials. However, the protein degraded before activity could be analyzed. Further co-expression trials were not able to reproduce these results; DmoA was overexpressed and little to no DmoB176 resulted.

Colony screening was performed in order to standardize a protocol for co-expression that would result in equal amounts of DmoB176 and DmoA each time. Although the DmoA protein was overexpressed in trials 2 and 3, the colonies from which it was grown contained only *dmoB176* according to PCR and gel electrophoresis. PCR conditions were analyzed to verify the primers, annealing temperatures, and BL21DE3 cell line would amplify the *dmoA* gene; PCR was consistently successful. Therefore, the reason as to why DmoA protein, but not *dmoA* gene, could be seen on a gel is currently unknown. Since stoichiometric co-expression was not reproducible, the ability to test activity was prevented; therefore, it is currently unknown whether co-expression of DmoA and DmoB176 has an effect on enzymatic function.

### *Future Works*

The main focus of future experimentation would be to obtain a consistent, reproducible co-expression protocol. This may include making competent cells containing one of the genes, or high-throughput protein expression screenings that result in expression of both DmoA and DmoB176. If the results of trial 1 are repeated glycerol stocks from that colony can be made.

Co-expression using the single vector approach may also need to be attempted.<sup>20</sup> This approach utilizes a single vector with different multiple cloning sites and separate promoters and ribosome binding sites. Once DmoA and DmoB176 are consistently co-expressed and purified in stoichiometric amounts, degradation of DMS can be tested towards the characterization of DMS monooxygenase. These studies will lay the ground work to understand how DMS degradation factors into the overall global sulfur cycle and climate regulation.

## **Financial Support**

Funding for this project has been provided by the Appalachian State University Office of Student Research, A. R. Smith Department of Chemistry, College of Arts & Sciences and the National Institute of Environmental Health Sciences.

## References

1. Andreae, M., et al. (1983) The biological production of dimethylsulfide in the ocean and its role in the global atmospheric budget *Ecological Bulletins* 35, 167-177.
2. Boden, R., et al. (2011) Purification and characterization of Dimethylsulfide Monooxygenase from *Hyphomicrobium sulfonivorans*. *J. Bacteriol.* 193(5), 1250-1258.
3. Chasteen, T. G.; Bentley, R. (2004) Volatile Organic Sulfur Compounds of Environmental Interest: Dimethyl Sulfide and Methanethiol. An Introductory Overview *Journal of Chemical Education* 81(10), 1524.
4. Climate Change and Infectious Disease. *Center for Health and the Global Environment*. Harvard School of Public Health.
5. Copeland, William C. (1997) Expression, purification, and characterization of the two human primase subunits and truncated complexes from *Escherichia coli* *Protein Expression and Purification* 9(1), 1-9.
6. Faloon, Ian (2009) Sulfur processing in the marine atmospheric boundary layer: A review and critical assessment of modeling uncertainties *Atmospheric Environment* 43, 2841-2854.
7. Fuyura, T., et al. (2003) Cloning of a gene encoding flavin reductase coupling with dibenzothiophene monooxygenase through coexpression screening using indigo production as selective indication *Biochemical and Biophysical Research Communications* 313, 570-575.
8. Harvell, C., et al. (2002) Climate warming and disease risks for terrestrial and marine biota *Science* 296 (5576), 2158-2162.
9. IPTG Induction Protein Expression - Introduction Principles (2017). *BiologicsCorp*. Biologics International.
10. Jeffers, C. E., et al. (2002) Complex formation between *Vibrio harveyi* luciferase and monomeric NADPH: FMN oxidoreductase, *Biochemistry* 42, 529-534.
11. Kimple ME, Brill AL, Parker RL (2013) Overview of Affinity Tags for Protein Purification. *Current protocols in protein science*.
12. Kravitz, B., et al. (2009) Sulfuric acid deposition from stratospheric geoengineering with sulfate aerosols *J. Geophys. Res.* 114, 1-7.
13. Lee, Pei Yun, et al. (2012) Agarose Gel Electrophoresis for the Separation of DNA Fragments *Journal of Visualized Experiments* 62, 3923.
14. Lodish H, Berk A, Zipursky SL, et al. *Molecular Cell Biology*. 4th edition. New York: W. H. Freeman; 2000. Section 7.1, DNA Cloning with Plasmid Vectors.
15. Mahmood, Tahrin, and Ping-Chang Yang (2012) Western Blot: Technique, Theory, and Trouble Shooting *North American Journal of Medical Sciences* 4.9, 429-434.
16. Ming, T., et al. (2014) Fighting global warming by climate engineering: Is the Earth radiation management and the solar radiation management any option for fighting climate change? *Renewable and Sustainable Energy Reviews* 31 792-834
17. Morgan, K. So Many Origins, So Little Time. *Plasmids 101: Origin of Replication*. Addgene.
18. Rasch, P., et al. (2008) An overview of geoengineering of climate using stratospheric sulphate aerosols *Phil. Trans. R. Soc. A* 366, 4007-4037.
19. Reisch, C. R., et al. (2011) Bacterial Catabolism of Dimethylsulfoniopropionate (DMSP) *Frontiers in Microbiology* 2.



20. Romier, C., et al. (2006) Co-expression of protein complexes in prokaryotic and eukaryotic hosts: experimental procedures, database tracking and case studies *Acta Cryst. D62*, 1232–1242.
21. Sathiamoorthy S, Shin JA (2012) Boundaries of the Origin of Replication: Creation of a pET-28a-Derived Vector with p15A Copy Control Allowing Compatible Coexistence with pET Vectors *PLoS ONE* 7(10), e47259.
22. Schafer, H., et al. (2010) Microbial degradation of dimethylsulphide and related C1-sulphur compounds: organisms and pathways controlling fluxes of sulphur in the biosphere *J. Exp. Botany* 61(2), 315-334.
23. van den Heuvel, R. H. H., et al. (2004) Structural studies on flavin reductase PheA2 reveal binding of NAD in an unusual folded conformation and support novel mechanism of action, *J. Biol. Chem.* 279, 12860-12867.
24. What is Geoengineering? *Oxford Geoengineering Programme*.